Cellulose Nanocrystals versus Polyethylene Glycol as Toughening Agents for Poly(Lactic Acid)-Poly(Acrylic Acid) Graft Copolymer

Jose Luis Orellana, Michael Mauhar and Christopher L. Kitchens*

Department of Chemical and Biomolecular Engineering, Clemson University, Clemson, South Carolina 29634, USA

ABSTRACT: Polylactic acid (PLA) is one of the most widely used biodegradable polymers due to the ability to synthesize it economically at industrial scale and its favorable properties for many consumer products. However, the rigid nature of PLA is not desirable for specific applications, requiring the incorporation of effective bio-derived additives in order to enhance the PLA toughness and broaden applications. In this work, PLA was modified by graft polymerization of polyacrylic acid (PLA-g-PAA) to increase the hydrophilicity to promote compatibilization of cellulose nanocrystals (CNCs) or high molecular polyethylene glycol (PEG). CNCs were found to act as a nucleating agent for the PLA-g-PAA copolymer due to an enhanced compatibility with these rigid nanocrystals, thus increasing the tensile modulus and reducing toughness. This was not the case for pure PLA, for which the toughness was increased up to 125% for a 1% CNC loading. PEG successfully increased toughness of the PLA-g-PAA by more than 34 times that of neat PLA and PLA-g-PAA with a substantial yet not critical reduction in strength and modulus for a wide range of applications.

KEYWORDS: Nanocomposites, cellulose nanowhiskers, plasticizers and crystallization

1 INTRODUCTION

Polylactic acid (PLA) is a biodegradable, bioabsorbable polymer derived from renewable resources, which offers promising alternatives to traditional petroleum-based plastics [1]. PLA, which accounts for 12.2% of bioplastics and 31% of the biodegradable plastics market [2], is utilized for applications ranging from medical devices to food packaging [3]. The tensile strength and elastic modulus of PLA is comparable to commodity polymers such as polyethylene terephthalate (PET); however, it has a very low toughness and elongation at break, limiting its widespread application [4]. To address these disadvantages, many additives and modifications, such as plasticizers [5, 6], fillers [7, 8], and graft copolymers [9, 10], have been investigated for PLA.

One of the primary challenges in the toughening of rigid polymers is to obtain a balance between the increase of toughness and reduction of tensile strength and modulus. In many cases, significant decreases in the strength

or modulus can result in poor performance, making the polymers unusable for intended applications [4]. For this reason, the balance of the properties is a key aspect of this type of investigation. In addition, many plasticizers are hydrophilic, representing issues of incompatibility with nonpolar matrices. Several approaches have received recent research attention, including a reactive modification of PLA with polyacrylic acid (PAA) and subsequent blending with polyethylene glycol (PEG), which successfully increased toughness without a significant loss in the tensile properties [11]. PEG, a hydrophilic, nontoxic polymer, is a common plasticizer that has been shown to increase the flexibility and ductility of polymers including PLA [12, 13]. However, the chemical incompatibility between PEG and PLA can drive the low molecular weight PEG to migrate and phase-separate from the matrix with time. On the other hand, the high molecular weight PEG is completely immiscible with the PLA matrix [14]. The miscibility of PEG in PLA can be improved by the grafting of PAA, which is more hydrophilic [11], potentially allowing improved miscibility with higher molecular weight PEG. Despite the best attempts to increase toughness without compromising tensile properties by enhancing chemical compatibility, the common trade-off between these two properties cannot be avoided when using

Corresponding author: ckitche@clemson.edu

PEG as a toughening agent. An alternative approach to enhance toughness without compromising tensile strength and modulus may be through the addition of cellulose nanocrystals.

Cellulose nanocrystals (CNCs), also known as cellulose nanowhiskers, have been widely investigated as reinforcement fillers for polymeric matrices due to their remarkable mechanical properties and high aspect ratios [15–17]. These fillers usually increase the modulus of the matrix through the addition of a rigid material and the formation of a percolating network; however, some research has reported an improvement in toughness without compromising other mechanical and thermal properties [18, 19]. In addition, research has also shown improved crystallinity and gas barrier properties for PLA with the addition of CNCs [20, 21], encompassing an increase in potential applications from food packaging to biomedical applications. One of the greatest challenges in the utilization of CNCs as a reinforcement filler for hydrophobic matrices is the hydrophilicity of native cellulose [22]. One approach to addressing this challenge is through the surface functionalization of the nanocrystals, either by covalent modification or the use of a surfactant compatibilizer [23].

In this work, the mechanical properties of PLA and PLA-g-PAA copolymer were improved by the addition of CNCs (1, 3, and 5 wt%) and high molecular weight PEG (10, 20 and 30 wt%). CNCs were isolated from cotton and functionalized by a combination of acetic acid and hydrochloric acid in order to produce acetylated CNCs. The mechanical properties were obtained using an Instron machine and the increase of toughness and modulus was observed depending on the combination of additives used. The self-assembly of the CNCs within the matrix was studied using polarized microscopy in order to understand the structure/property relationship of the nanocomposites. The plasticizing efficiency of PEG was evaluated by the shift of glass transition temperature (Tg) measured using differential scanning calorimetry.

2 MATERIALS AND METHODS

2.1 Materials

Polylactic acid (PLA) 2002D was purchased from NatureWorks LLC ($M_w \approx 198$ kDa and $M_n \approx 76$ kDa) [24]. Benzyl peroxide was purchased from FLUKA. Acrylic acid 99% and 10 kDa polyethylene glycol (PEG) (OH-terminated) were obtained through Aldrich. Cotton ashless powder from Whatman was used as the source of cellulose. All other solvents and reactants in this work were ACS grades obtained from VWR.

2.2 Preparation of Cellulose Nanocrystals

Cellulose nanocrystals were isolated by acid hydrolysis with a mixture of hydrochloric acid (HCl) and acetic acid (AA) as developed by Dorgan and coworkers [25]. In this reaction, a Fischer esterification reaction occurs between the hydroxyl groups and the acetic acid during the hydrolysis, introducing methylesters onto the CNC surface. For the isolation, 10 g of cotton were soaked for approximately 12 h in a round-bottom flask with 225 mL of AA. The next day, 24.5 mL of DI water and 0.8 mL 37% HCl were added. The reaction was conducted for 10 h at 105 °C with constant stirring and stopped cooling in an ice bath. Three washes with DI water were carried out by sequential centrifugation (8,600 rpm for 3 min) and vortex mixing to remove the remaining acid from the cellulose. The suspension was combined and ultra-sonicated in an ice bath using a Fisher Scientific 550 Sonic Dismembrator for 35 min (5 cycles of 7 min pulse, 2 min rest) at a power level of 7.5. The suspension was washed again two more times and the resulting supernatant was combined and stored as the CNC stock suspension. To transfer the CNCs to an organic solvent, the supernatant was precipitated by centrifugation at 14,000 rpm for 10 min, washed twice with acetone to remove bound water, and transferred to chloroform. The suspension was agitated vigorously in a vortex mixer until no CNC agglomerates were observed.

2.3 PLA Reactive Modification and Blending

The PLA reactive modification was performed in a 1 L Parr reactor to produce a graft copolymer with 10 wt% PAA. The PAA side chains were grafted from the PLA polymer chains using benzoyl peroxide as an initiator as described by Rasal and Hirt [11]. Initially, the reactor was loaded with 100 g of PLA and dissolved in 750 mL of chloroform with constant agitation at 100 rpm. Benzoyl peroxide totaling 1% of the mass of PLA was added to the initial solution in the reactor. The reactor was sealed and heated to 60 °C for 60 min. The heater was turned off and 10 g of acrylic acid were added to the solution. The reactor was resealed and heated to 100 °C for 10 min. The heater was shut off and the reactor was allowed to cool to below 60 °C before the solution was drained from the bottom of the reactor. This solution was then separated into specific portions before the desired amount of CNCs or PEG was added to the mixture. This solution was thoroughly blended with an overhead impeller for 10 min and then poured out in a Pyrex dish. The chloroform was allowed to evaporate in a hood overnight followed by 24 h at 80 °C under vacuum. The resulting films were cut into approximately 5 mm squares in preparation for extrusion.

A sample film of the reactively modified PLA-PAA without any co-polymer or toughening agents was tested with a Nicolet Avatar 360 Fourier transform infrared spectroscopy instrument to verify the presence of acrylic acid side chains. This film was submerged in DI water and held at 70 °C for 60 min in a Mars 5 microwave accelerated extraction machine. After microwave extraction, this film was again tested with FTIR to verify that the acrylic acid side chains had chemically grafted onto the PLA matrix, and were not just part of the polymeric mixture.

2.4   Film Extrusion

The polymer films were extruded using a twin-screw micro-compounder (DSM Xplore®, from The Netherlands) operating in co-rotating mode with 170-mm-long tapered screws and a barrel volume of 15 cm³. The polymer was compounded for approximately 10 min at 180 °C with the motor force set to 500 N and the rate of co-rotating screws controlled by the instrument. The polymer melt was extruded through a rectangular cross-sectional shape die and cooled by ambient nitrogen. The resulting films were approximately 0.1 mm thick and collected on a chill roll at a take-up speed between 110 to 130 rpm depending on the viscosity of the melt. These films were diced into uniform strips 95 mm long and 12.5 mm wide on a USM hydraulic machine press by means of a metal die. The thickness of each film was measured at 4 different points with a film thickness gauge (Digimacro ME-50HA).

2.5   Characterization of Films

Tensile testing of the polymer film strips was conducted using an Instron 1125 universal testing instrument. The initial grip separation was set to 45 mm and a crosshead speed of 4 mm/min in compliance with the ASTM 882 standard. All mechanical testing was done only in the direction of extrusion. The stress-strain curves were analyzed with Origin® software in order to determine the tensile strength, tensile modulus, and toughness of each film.

Differential scanning calorimetry (DSC) (TA Instruments DSC 2920) was used to measure the thermal transitions: glass transition temperature (T_g), crystallization temperature (T_c), melting temperature (T_m), and the heat of crystallization (ΔH_{cc}) and melting (ΔH_m), and percent crystallinity of the films (X_c). Aluminum pans were carefully loaded and sealed with 4 to 6 mg of the polymer sample and heated to 200 °C at a constant rate of 10 °C/min under a nitrogen purge. At the end of the run, the samples were cooled by quenching using a metal bar previously submerged in liquid nitrogen.

A second run was immediately conducted on these samples under the same conditions. T_g, T_c, T_m, ΔH_{cc} and ΔH_m, were taken from the second run after quenching. The X_c of the nanocomposites was determined from the first run before quenching using Equation 1,

$$X_c\,[\%] = \frac{\Delta H_m - \Delta H_{cc}}{\left(\Delta H_m^{\infty}\right) \times W_{PLA}} \times 100\% \qquad (1)$$

where W_{PLA} is the fraction of PLA in the composites, and ΔH_m^{∞} is the theoretical enthalpy of fusion of 100% crystalline PLA, which was taken to be 93.0 J/g [20].

Optical polarized-light microscopy was performed using an Olympus BX-60 in transmission mode with a polarizer in the bottom of the sample and the analyzer rotated 90° in the top. A first order red plate (U-TP530) was also used to study the specific orientation of the organized crystals. The samples were placed on a glass microscope slide without further preparation and photos were taken at rotating angles of 0, 45, 90 and 135° using 13X magnification.

3   RESULTS AND DISCUSSION

The PLA was reactively modified with acrylic acid by means of the initiator benzyl peroxide as detailed in the literature [11]. The reaction took place at elevated temperatures in a sealed reactor, producing a graft copolymer with 10 wt% PAA, hereafter referred to as PLA-g-PAA. The copolymer was analyzed to verify the covalent attachment of PAA onto PLA using FTIR analysis after microwave extraction of the PLA-g-PAA(10%) in water. CNCs or PEG were added in the desired concentrations and physically mixed in solution to form the nanocomposites or polymer blends, respectively. Nanocomposites of pure PLA were also prepared in order to compare the effects with the graft copolymer.

3.1   PLA and PLA-g-PAA Nanocomposites

3.1.1   Mechanical Properties

Figure 1 shows the tensile toughness, tensile strength, and tensile modulus of the PLA and PLA-g-PAA nanocomposites films. The addition of CNCs to the PLA films resulted in increased toughness as observed in Figure 1: increasing from 1.1 MJ/m³ for neat PLA to a maximum of 2.5 MJ/m³ (125% increase) at 1% CNC load. At higher CNC loadings, the toughness progressively decreased to a lowest value of 1.6 MJ/m³ for 5% CNC, which still represented a 46% increase over the neat PLA. For the PLA-g-PAA, the toughness decreased as the CNC load increased, obtaining a lowest value at 5% CNC load, which represented a 75%
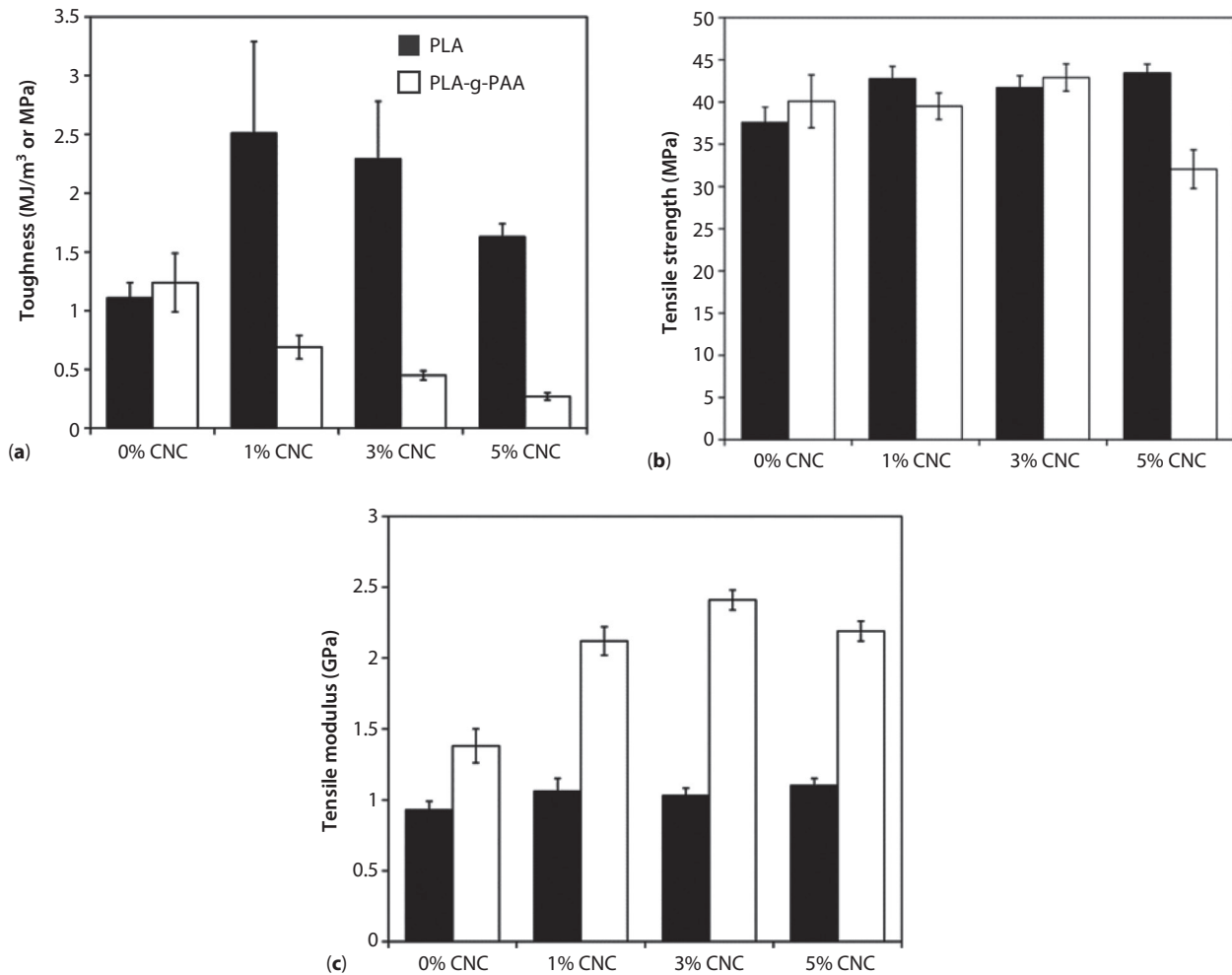
Figure 1 Mechanical properties of PLA (■) and PLA-g-PAA/CNC (□) nanocomposites: (**a**) toughness, (**b**) tensile strength, and (**c**) tensile modulus.

decrease. The tensile strength (Figure 1b) for both PLA and PLA-g-PAA only increased slightly with the addition of CNCs, as was the case for the tensile modulus of PLA (Figure 1c). On the other hand, the modulus of the PLA-g-PAA composites was enhanced for all the CNC concentrations, having an optimum increase of 3% CNC, representing a 159% increase.

The interfacial interactions between CNCs and the matrix play a very important role in the reinforcement of the mechanical properties, especially in the toughness, which has been shown to increase due to strong filler-matrix interactions in CNC nanocomposites [26]. On the other hand, a lower compatibility between CNCs and the matrix allows the filler to associate with itself, forming a rigid percolating network which can be responsible for the enhancement of the modulus [23]. This network is frequently formed when there is a balance of surface charge and hydrogen bonding, since only strong electrostatic attractions tend to favor the formation of agglomerates [27]. In addition,

the theoretical critical volume fraction at which the network would begin to form is 9 vol% (11 wt%) for the CNCs isolated in this work, as predicted by Favier *et al.* for cylindrical shaped particles [28]. Therefore, it is unlikely that the increase in modulus of the PLA- g-PAA nanocomposites is due to such a network.

Another possible reason for the increase of the PLA-g-PAA modulus is a higher crystallinity obtained upon the addition of CNCs. Several publications have reported the increase of crystallinity upon addition of nanocellulose to polymers including PLA, resulting in higher tensile strength and modulus [20, 29]. Pei *et al.* reported that surface-modified CNCs promoted higher crystallinities and tensile properties than unmodified CNCs in PLA [20].

3.1.2 Thermal Properties of Nanocomposites

The results in Table 1 show an increase in PLA-g-PAA crystallinity from 33.1% for neat copolymer to 48.9%

Table 1 Thermal properties of PLA and PLA-g-PAA loaded with cellulose nanocrystals.

Polymer	CNC (wt%)	T_g (°C)	T_{cc} (°C)	T_m (°C)	ΔH_{cc} (J/g)	ΔH_m (J/g)	$X_{c\,1st\,run}$ (%)	$X_{c\,2nd\,run}$ (%)
PLA-CNC	0	55.5	122.1	149.9	26.2	26.6	28.3	0.4
	1	55.8	123.6	150.4	25.4	26.4	30.6	1.1
	3	58.1	132.6	153.4	4.0	3.3	28.2	0.0
	5	57.9	134.9	153.3	2.7	2.8	29.3	0.2
PLA-g-PAA-CNC	0	56.9	132.2	147.7	4.0	6.4	33.1	2.8
	1	57.2	132.9	152.1	5.1	7.7	36.5	3.2
	3	57.1	131.2	152.3	10.2	10.7	48.9	0.7
	5	56.3	132.3	152.0	6.0	6.5	35.3	0.7
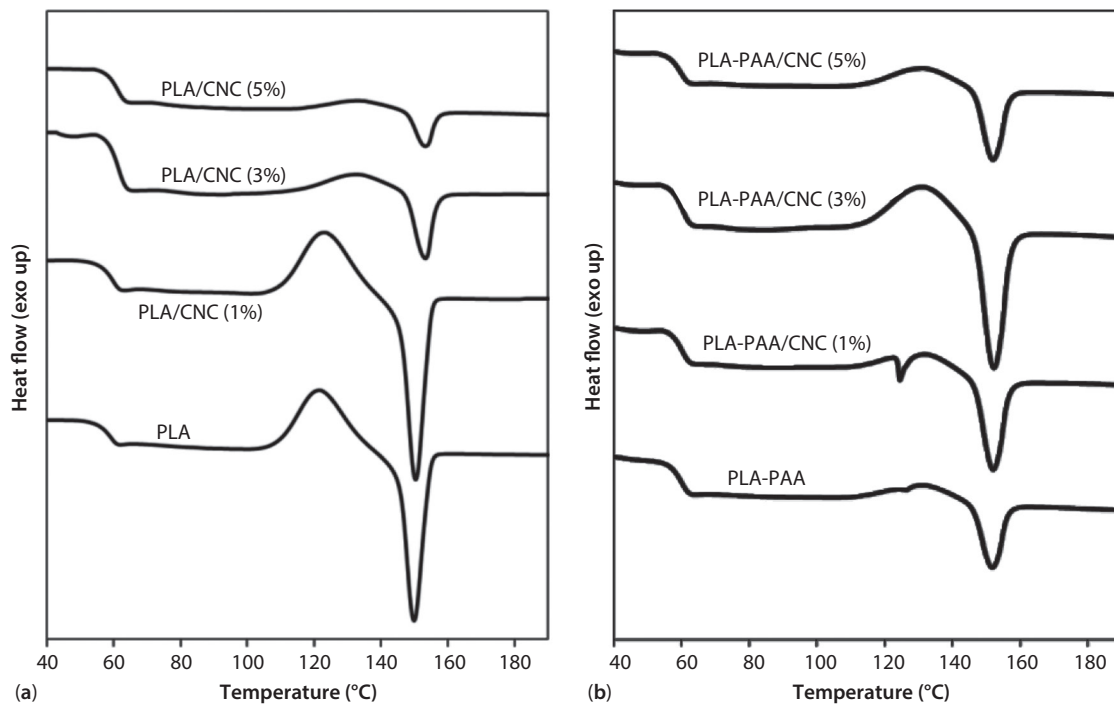
Figure 2 Second run DSC scan curves of PLA (**a**) and PLA-g-PAA (**b**) loaded with cellulose nanocrystals. The plots are offset for clarity.

at 3% CNC load, before suffering a slight reduction at 5% CNCs. These results correlate well with the enhancement of modulus as discussed above. Hence, the grafting of the hydrophilic PAA into PLA increases the compatibility with CNCs [30], which results in improved CNC dispersion and the nanocrystals acting as effective nucleating agents for the copolymer. For the PLA composites, CNC addition did not show a significant increase in crystallinity, which parallels the lack of increased tensile modulus for these composites.

The DSC results obtained from the second run after quenching are shown in Figure 2. For PLA composites (Figure 2a), the area of the exothermic peak attributed to the cold crystallization gradually decreased with increasing CNC concentration, while the peak for the PLA-g-PAA composites increased (Figure 2b). The melting temperature (T_m) and the glass transition temperature (T_g) had the tendency to increase with CNC concentration in both cases. The values of these thermal transitions are shown in Table 1. The slight increase in the T_g of the PLA nanocomposites could be evidence of reduced mobility of the chains, either due to increased crystallinity in the polymer or chain entanglements on the nanofiller [31]. However, since the crystallinity of PLA composites did not increase, this increase of T_g can be attributed to the chain entanglement around the CNC. This translates to higher energies to obtain the same mobility of the polymer under stress, and correlates with the increase in toughness obtained for PLA composites as shown in Figure 1a.

The reduced mobility of PLA chains upon addition of CNCs is also reflected in the significant reduction of the second run heat of crystallization, and consequently in the heat of melting for the PLA composites. This is contrary to the PLA-g-PAA copolymers which increased their mobility due to an improved crystallization as observed in Table 1. This difference in the crystallization between both types of polymers may be based on the strength of the interactions and the starting state of the material. As observed in Table 1, the heat of crystallization for neat PLA is much higher than for the PLA-g-PAA. The addition of CNCs actually disrupts the initial mobility of PLA chains, while for hydrophilic PLA-g-PAA, CNCs may enhance the initially low crystallization of this copolymer due to an increased compatibility. Liu *et al.* also found that the crystallization of PLA was more effective in the amorphous polymers than in the crystalline ones upon the addition of CNCs [29].

3.1.3 Optical Properties

Previous research has shown that the nanostructure of CNCs in nanocomposites is a key determining factor on the mechanical properties [32]. A spiral formation was shown to contribute to the increase of toughness of the composites when using sulfuric acid-synthesized CNCs, which is similar to the behavior observed in the fibers of plants and trees [33]. For this reason, the optical properties of the films were studied using polarized-light microscopy in the present work. The polarizer, which was placed under the sample, was aligned along the 0° angle (north-south direction), while the analyzer, which is above the sample, was at the 90° angle (east-west). Figure 3 shows the polarized micrographs of the PLA and PLA-g-PAA composites rotated at 0°, 45°, 90° and 135° angles. For the PLA composites, a bright phase or birefringence can be observed at 45° and 135° angles, indicating the formation of liquid crystals either parallel or perpendicular to the direction of extrusion. The birefringence is significantly brighter for the 3% CNC in PLA, indicating the formation of an ordered liquid crystalline phase, and therefore a greater degree of CNC self-assembly within the matrix. The formation of an oriented phase in a matrix is usually a good indication of non-agglomerated nanocrystals [34, 35], which agrees
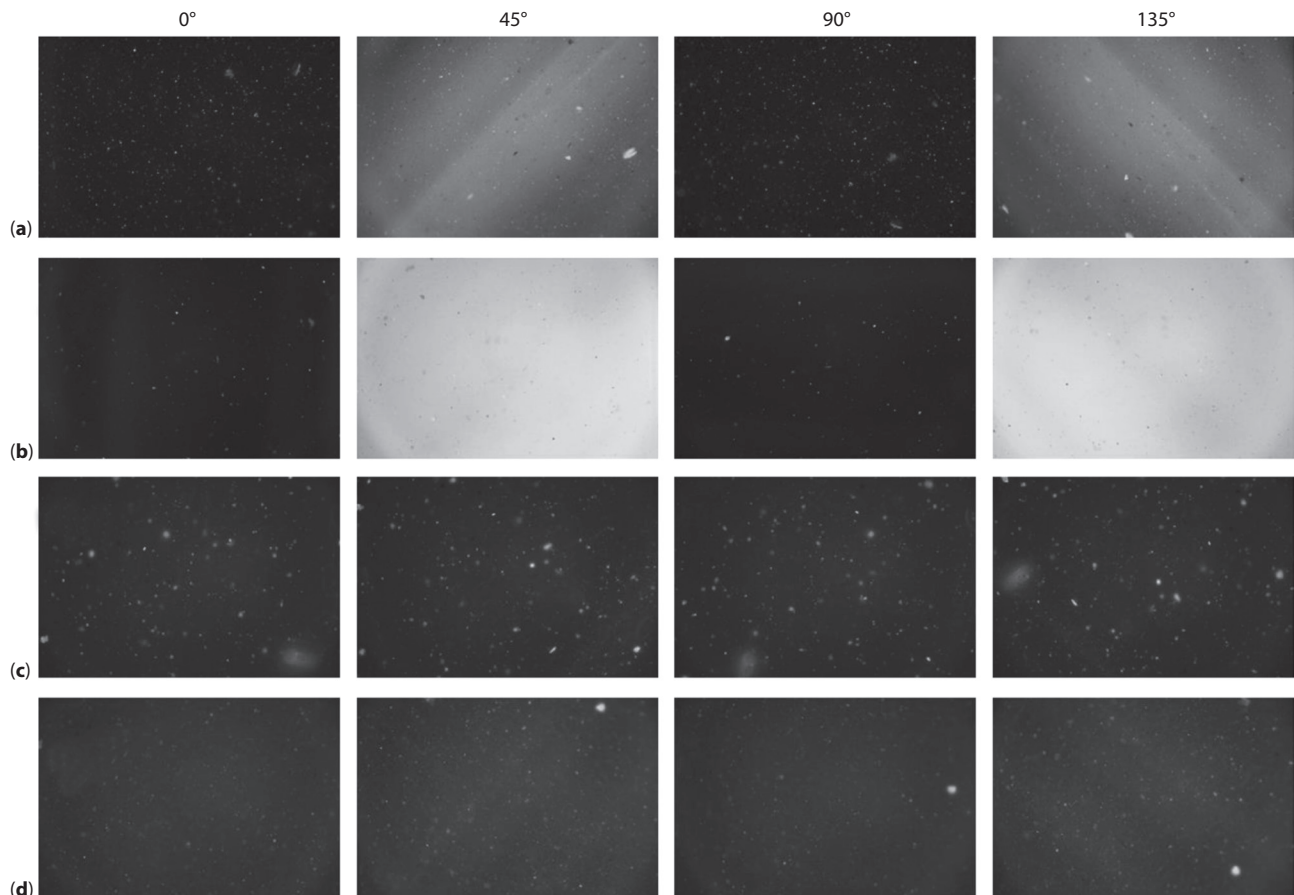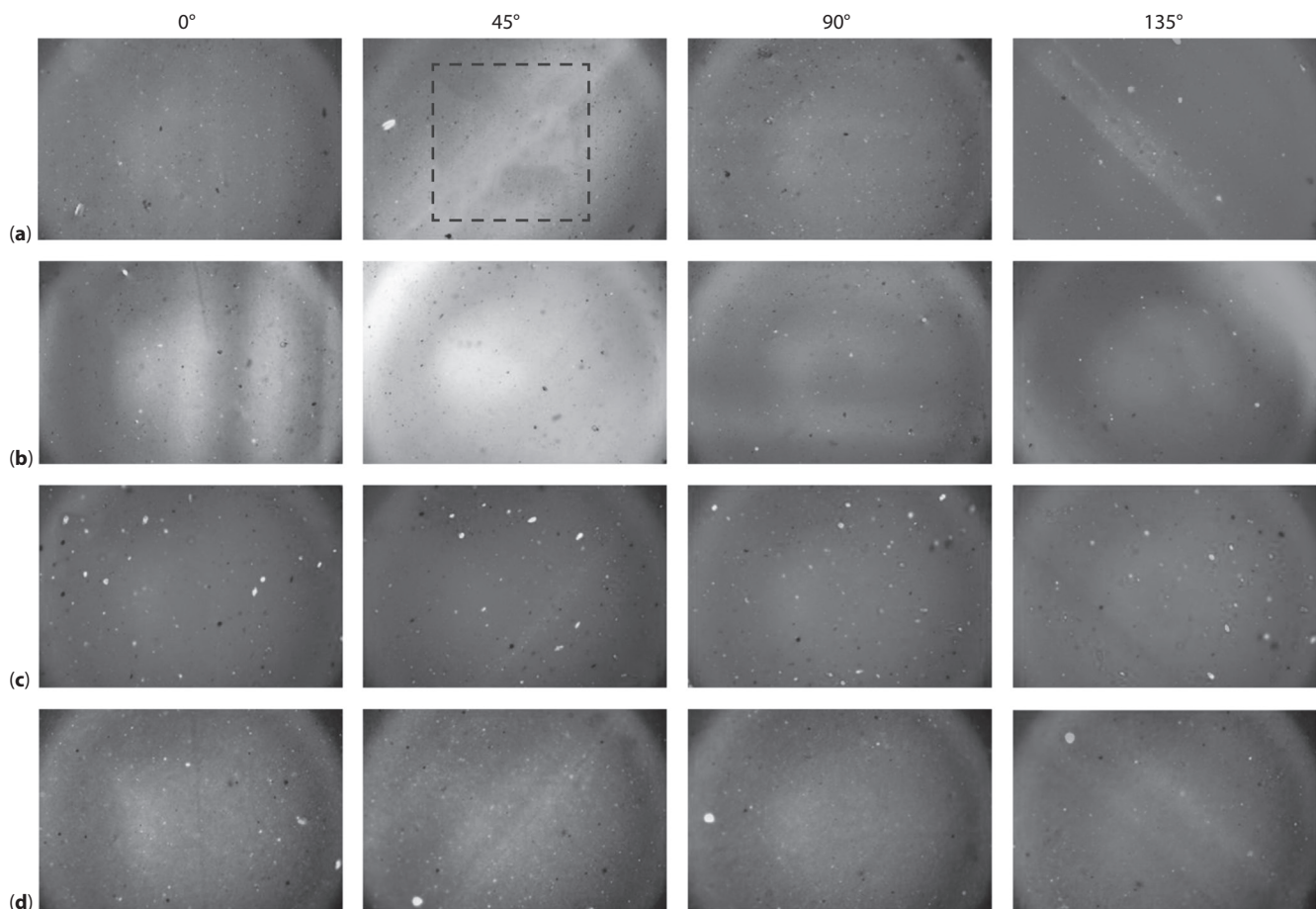

Figure 3 Polarized-light microscopy of PLA (**a**, **b**) and PLA-g-PAA/CNC nanocomposites (**c**, **d**). (**a**, **c**) 1% and (**b**, **d**) 3% CNC. Length of each image: 1.5 mm.

with the theory of the enhancement of toughness due to dispersed and more compatible fillers. On the contrary, an oriented phase is not observed for the PLA-g-PAA nanocomposites, which may be attributed to CNCs association with the stiff PAA chains and PLA crystallites that inhibit the self-assembly of the nanocrystals.

A first order red plate was used to determine the specific orientation of the assembled crystals and the results are shown in Figure 4. The slow axis of the plate was placed parallel to the 135° angle (northwest-southeast), and the direction of the extrusion of the films was always parallel to the rotation angle. The appearance of the color magenta, yellow, and blue are indicative of the different orientations of the assemblies. CNCs oriented in the 135° angle will present a color blue, while the assemblies oriented in the 45° angle will be yellow. Magenta colors indicate the alignment at 0°, 90°, and also the unoriented

nanocrystals. Hence, the total theoretical oriented area of the films can be estimated by adding the percentage of both yellow and blue from 2 consecutive angles of rotation.

The percentage of the oriented area for the PLA composites, estimated from a centered region of the obtained images, increased from 85% to 100% for the 1% and 3% CNC loadings, respectively. For the PLA-g-PAA composites, the oriented area only increased from 2% to 4% for the 1% and 3% CNC composites, respectively. The directions of the crystal assemblies are predominately parallel to the direction of the extrusion, which is demonstrated for the amount of yellow for the 45° rotation angle. For the PLA-CNC 1% films, approximately 75% of the CNCs is estimated to be oriented parallel to the line of extrusion, while for the PLA-CNC 3% films the orientation is apparently more than 100%. This > 100% value, however, lacks significant meaning other than very high organization

Figure 4 Polarized-light microscopy PLA (**a**, **b**) and PLA-g-PAA/CNC nanocomposites (**c**, **d**) using a first order red filter. (**a**, **c**) 1% and (**b**, **d**) 3% CNC nanocomposites. The dotted square in the picture represents the size of the area used for the color quantification. Length of each image: 1.5 mm.

because the birefringence of this composite is too bright as observed in Figure 3, as the red plate is not designed for the analysis of such high levels of retardation.

3.2 PLA-g-PAA Copolymer Blends

PEG was added to the PLA-g-PAA graft copolymer in solution immediately after the reaction of acrylic acid with PLA. Neat PLA blended with PEG was not prepared since it has already been studied in the literature [13, 36–39]. The study of low molecular weight (<2 kDa) PEG is commonly studied because at high molecular weights phase separation [13] and reduction in tensile properties [40] occur due to immiscibility between the components. However, low molecular weight plasticizers have the tendency to migrate from the host polymer due to a slow phase separation and the crystallization of PEG at room temperature [14, 41]. This problem can be addressed by increasing the compatibility with grafting of PAA onto the hydrophobic PLA matrix [11]. PAA and PEG are both hydrophilic polymers and are more compatible with each other than with PLA. Previous research investigated this reactive-blend modification using a low molecular weight PEG (Mn = 1.5kDa), obtaining a significant increase in toughness without compromising the tensile properties of the films [11]. In this work, a higher molecular weight PEG (10 kDa) was blended with the graft copolymer to explore the enhancement of PLA properties with possible reduced migration rates of the plasticizer.

3.2.1 Mechanical Properties

The mechanical properties of the PLA-g-PAA/PEG blends (0, 10, 20 and 30% PEG) were determined from the stress-strain curves and are shown in Figure 5. It can be observed that the toughness was greatly increased as the percentage of PEG was increased in the formulation. The highest toughness was reached at 30% PEG (39.9 MJ/m^3), increasing by 34 times that of PLA (1.1 MJ/m^3) and PLA-g-PAA (1.2 MJ/m^3). For 10% and 20% PEG, the toughness was increased 10 fold (11.4 MJ/m^3) and 25 fold (27.5 MJ/m^3) respectively.

The tensile properties of the blends are shown in Figure 5b,c. PAA grafting increased the strength and the modulus of the graft copolymer by 7% and 48%, respectively, due to the higher stiffness of PAA. The addition of PEG decreased both the tensile strength and modulus of the films with similar trends. The tensile strength was reduced as much as 49% for the 20% PEG, while the modulus decreased 30.1% for the 30% PEG content, which is a common behavior observed in the plasticization of polymers.
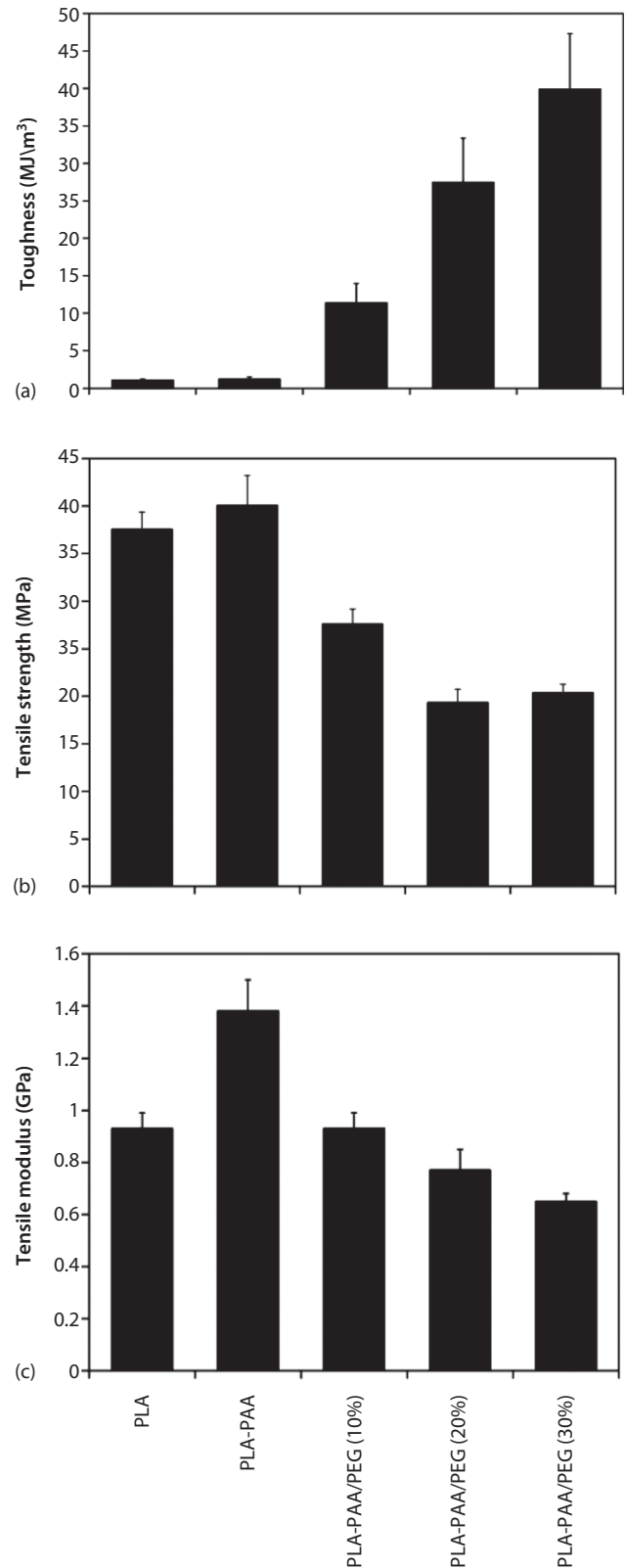
Figure 5 Mechanical properties of PLA-g-PAA/PEG blends: (**a**) toughness, (**b**) tensile strength, and (**c**) tensile modulus.
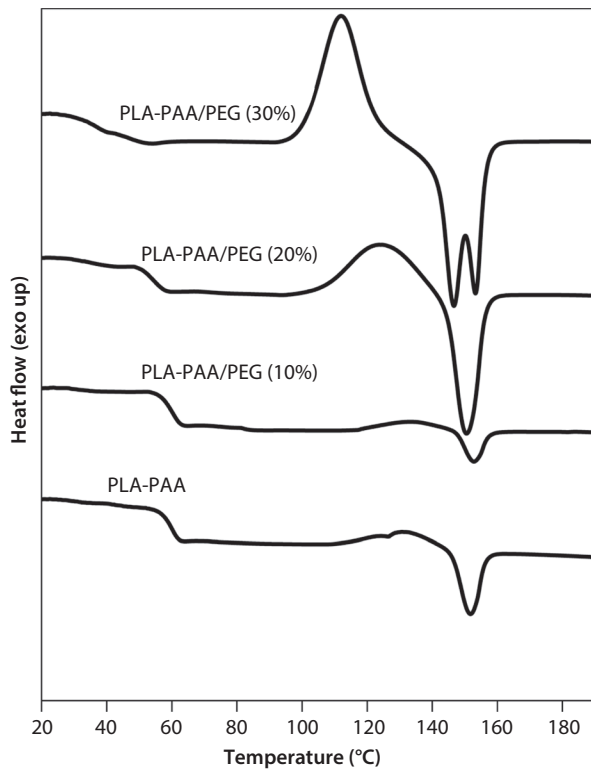
Figure 6 Second run DSC curves of PLA-g-PAA/PEG blends.

Table 2 Thermal properties of PLA-g-PAA blends.

PEG (wt%)	T_g (°C)	T_{cc} (°C)	T_m (°C)	ΔH_{cc} (J/g)	ΔH_m (J/g)	X_c (%)
0	56.9	132.22	147.7	4.022	6.4	32.4
10	56.4	133.09	153.3	2.403	2.3	48.0
20	50.2	123.93	150.1	14.86	14.2	36.9
30	30.9	112.05	152.3	24.26	25.5	38.2

3.2.2 Thermal Properties

The DSC plots for the PLA-g-PAA/PEG blends after quenching are shown in Figure 6. The plots show the endothermic melting peaks in all of the blends and an increasing endothermic crystallization peak with PEG concentration. A double peak can be observed during the melting region for the 30% PEG blend, which has been attributed to lamellar rearregement during crystallization of PLA [42]. The efficiency of plasticization can be evaluated by the T_g decrease, which went from 56.9 °C for neat PLA-g-PAA to 30.9 °C for a 30% PEG formulation as observed in Table 2. Moreover, a reasonable miscibility of the blend is suggested by the appereance of a single T_g transition and by the lowering of this value with increasing plasticizer content for concentrations lower than 30%. The change in Tg

for 30% PEG is significant; however, there is not evidence of phase separation at this level of plasticizing. The heat of crystallization and melting increased with the addition of PEG, demonstrating increased mobility of the PLA chains due to the plasticizing effect of PEG [6]. This behavior also indicates higher crystallization rates, which are beneficial due to the slow crystallization kinetics of PLA when it is cooled from the melt [43].

4 CONCLUSIONS

The toughening of PLA was achieved by the addition of either acetylated CNCs or PEG, and both were shown to act as toughening agents for PLA and PLA-g-PAA copolymer, respectively. Polyacrylic acid (PAA) was grafted onto PLA to increase the hydrophilicity of the polymer and to improve the compatibility of the reinforcements. CNCs increased the toughness of PLA by 125% with an optimum loading of 1% without compromising the tensile strength and modulus. This increase was attributed to two effects: chain entanglements on the nanocrystals and self-assembly on the CNC in the PLA matrix. For the PLA-g-PAA composites, the toughness decreased, while the modulus increased significantly with CNC concentration. This behavior was attributed to an increase of crystallinity of the PLA-g-PAA composites as a result of increased compatibility between CNCs and the PAA chains.

The thermal properties of these nanocomposites revealed a lower mobility for both the PLA and PLA-g-PAA chains as reflected by the slight increase of Tg. This reduced mobility was attributed to the increase of crystallinity for the PLA-g-PAA composites, while for PLA, it was attributed to polymer chain entanglements on the nanocrystals. These two effects correspond correctly with the enhancement of mechanical properties observed in both types of polymers. PLA composites exhibited a greater degree of CNC orientation compared to PLA-g-PAA as observed under polarized microscopy, suggesting the self-assembly of the CNCs in PLA. This assembly was found to be less oriented around the extrusion line for the 1% CNC films, which also exhibited enhanced toughness, compared to the 3% CNC composites of PLA.

High molecular weight PEG greatly increased the toughness of PLA-g-PAA copolymer by approximately 36 times, decreasing the tensile strength and tensile modulus only 49% and 30%, respectively, for the same PEG content. The Tg was decreased by 26 °C, demonstrating an effective plasticization when using 30% PEG. Moreover, the appearance of single T_g transition also indicated favorable miscibility for the blends. It can be expected that tuning the concentrations of PLA, PLA-g-PAA, CNCs, and PEG may enable the design

of a polymer composite with desired combinations of mechanical, optical, and thermal properties, thus expanding potential application for the bio-based composites.

Acknowledgments

References

1. J. Ahmed and S.K. Varshney, Polylactides-chemistry, properties and green packaging technology: A review. *Int. J. Food Prop.* **14,** 37–58 (2011).

2. European Bioplastics Assn., Bioplastics facts and figures, in: *European Bioplastics,* http://docs.european-bioplastics.org/2016/publications/EUBP_facts_and_figures.pdf. (2016).

3. K.M. Nampoothiri, N.R. Nair, and R.P. John, An overview of the recent developments in polylactide (PLA) research. *Bioresource Technol.* **101,** 8493–8501 (2010).

4. K.S. Anderson, K.M. Schreck, and M.A. Hillmyer, Toughening polylactide. *Polym. Rev.* **48,** 85–108 (2008).

5. K. Sungsanit, N. Kao, and S.N. Bhattacharya, Properties of linear poly(lactic acid)/polyethylene glycol blends. *Polym. Eng. Sci.* **52,** 108–116 (2012).

6. O. Martin and L. Averous, Poly(lactic acid): Plasticization and properties of biodegradable multiphase systems. *Polymer* **42,** 6209–6219 (2001).

7. G. Siqueira, J. Bras, and A. Dufresne, Cellulosic bionanocomposites: A review of preparation, properties and applications. *Polymers* **2,** 728–765 (2010).

8. S.S. Ray, Polylactide-based bionanocomposites: A promising class of hybrid materials. *Acc. Chem. Res.* **45,** 1710–1720 (2012).

9. H.I. Oyama, Super-tough poly(lactic acid) materials: Reactive blending with ethylene copolymer. *Polymer* **50,** 747–751 (2009).

10. G. Theryo, F. Jing, L.M. Pitet, and M.A. Hillmyer, Tough polylactide graft copolymers. *Macromolecules* **43,** 7394–7397 (2010).

11. R.M. Rasal, D.E. Hirt, Poly(lactic acid) toughening with a better balance of properties. *Macromol. Mater. Eng.* **295,** 204–209 (2010).

12. H.Z. Liu and J.W. Zhang, Research progress in toughening modification of poly(lactic acid). *J. Polym. Sci. B-Polym. Phys.* **49,** 1051–1083 (2011).

13. B.-S. Park, J.C. Song, D.H. Park, and K.-B. Yoon, PLA/chain-extended peg blends with improved ductility. *J. Appl. Polym. Sci.* **123,** 2360–2367 (2012).

14. X. Ran, Z. Jia, C. Han, Y. Yang, and L. Dong, Thermal and mechanical properties of blends of polylactide and poly (ethylene glycol-co-propylene glycol): Influence of annealing. *J. Appl. Polym. Sci.* **116,** 2050–2057 (2010).

15. M. Jamshidian, E.A. Tehrany, M. Imran, M. Jacquot, and S. Desobry, Poly-lactic acid: Production, applications, nanocomposites, and release studies. *Compr. Rev. Food. Sci. Food Saf.* **9,** 552–571 (2010).

16. S.J. Eichhorn, A. Dufresne, M. Aranguren, N.E. Marcovich, J.R. Capadona, S.J. Rowan, *et al.*, Review: Current international research into cellulose nanofibres and nanocomposites. *J. Mater. Sci.* **45,** 1–33 (2010).

17. E.E. Urena-Benavides, P.J. Brown, and C.L. Kitchens, Effect of jet stretch and particle load on cellulose nanocrystal-alginate nanocomposite fibers. *Langmuir* **26,** 14263–14270 (2010).

18. M. Bulota, K. Kreitsmann, M. Hughes, and J. Paltakari, Acetylated microfibrillated cellulose as a toughening agent in poly (lactic acid). *J. Appl. Polym. Sci.* **126,** E448–E457 (2012).

19. D. Bondeson and K. Oksman, Dispersion and characteristics of surfactant modified cellulose whiskers nanocomposites. *Compos. Interface.* **14,** 617–630 (2007).

20. A. Pei, Q. Zhou, and L.A. Berglund, Functionalized cellulose nanocrystals as biobased nucleation agents in poly (L-lactide) (PLLA)—Crystallization and mechanical property effects. *Compos. Sci. Technol.* **70,** 815–821 (2010).

21. H. Fukuzumi, T. Saito, T. Wata, Y. Kumamoto, and A. Isogai, Transparent and high gas barrier films of cellulose nanofibers prepared by TEMPO-mediated oxidation. *Biomacromolecules* **10,** 162–165 (2009).

22. S. Kalia, A. Dufresne, B.M. Cherian, B.S. Kaith, L. Averous, J. Njuguna, and E. Nassiopoulos, Cellulose-based bio- and nanocomposites: A review. *Int. J. Polym. Sci.* **2011,** Article ID 837875 (2011).

23. Y. Habibi, L.A. Lucia, O.J. Rojas, Cellulose nanocrystals: Chemistry, self-assembly, and applications. *Chem. Rev.* **110,** 3479–3500 (2010).

24. J. Cailloux, O. Santana, E. Franco-Urquiza, J. Bou, F. Carrasco, J. Gámez-Pérez, and M. Maspoch, Sheets of branched poly (lactic acid) obtained by one step reactive extrusion calendering process: Melt rheology analysis. *Express Polym. Lett.* **7,** 304–318 (2013).

25. B. Braun and J.R. Dorgan, Single-step method for the isolation and surface functionalization of cellulosic nanowhiskers. *Biomacromolecules* **10,** 334–341 (2009).

26. E.E. Urena-Benavides and C.L. Kitchens, Wide-angle X-ray diffraction of cellulose nanocrystal-alginate nanocomposite fibers. *Macromolecules* **44,** 3478–3484 (2011).

27. R. Rusli, K. Shanmuganathan, S.J. Rowan, C. Weder, and S.J. Eichhorn, Stress transfer in cellulose nanowhisker composites-influence of whisker aspect ratio and surface charge. *Biomacromolecules* **12,** 1363–1369 (2011).

28. V. Favier, G.R. Canova, S.C. Shrivastava, and J.Y. Cavaille, Mechanical percolation in cellulose whisker nanocomposites. *Polym. Eng. Sci.* **37,** 1732–1739 (1997).

29. D.Y. Liu, X.W. Yuan, D. Bhattacharyya, and A.J. Easteal, Characterisation of solution cast cellulose nanofibre-reinforced poly(lactic acid). *Express Polym. Lett.* **4,** 26–31 (2010).

30. P. Lu and Y.-L. Hsieh, Cellulose nanocrystal-filled poly (acrylic acid) nanocomposite fibrous membranes. *Nanotechnology* **20,** 415604 (2009).

31. X.Z. Xu, F. Liu, L. Jiang, J.Y. Zhu, D. Haagenson, and D.P. Wiesenborn, Cellulose nanocrystals vs. cellulose nanofibrils: A comparative study on their microstructures and effects as polymer reinforcing agents. *ACS Appl. Mater. Interfaces* **5,** 2999–3009 (2013).

32. E.E. Urena-Benavides and C.L. Kitchens, Cellulose nanocrystal reinforced alginate fibers-biomimicry meets polymer processing. *Mol. Cryst. Liq. Cryst.* **556,** 275–287 (2012).

33. J. Barnett and V.A. Bonham, Cellulose microfibril angle in the cell wall of wood fibres. *Biol. Rev.* **79,** 461–472 (2004).

34. L. Heux, G. Chauve, and C. Bonini, Nonflocculating and chiral-nematic self-ordering of cellulose microcrystals suspensions in nonpolar solvents. *Langmuir* **16,** 8210–8212 (2000).

35. J. Araki, Electrostatic or steric?—preparations and characterizations of well-dispersed systems containing rod-like nanowhiskers of crystalline polysaccharides. *Soft Matter* **9,** 4125–4141 (2013).

36. Z. Gui, Y. Xu, Y. Gao, C. Lu, and S. Cheng, Novel polyethylene glycol-based polyester-toughened polylactide. *Mater. Lett.* **71,** 63–65 (2012).

37. S. Jacobsen and H.G. Fritz, Plasticizing polylactide—The effect of different plasticizers on the mechanical properties. *Polym. Eng. Sci.* **39,** 1303–1310 (1999).

38. Z. Kulinski and E. Piorkowska, Crystallization, structure and properties of plasticized poly(L-lactide). *Polymer* **46,** 10290–10300 (2005).

39. I. Pillin, N. Montrelay, and Y. Grohens, Thermo-mechanical characterization of plasticized PLA: Is the miscibility the only significant factor?. *Polymer* **47,** 4676–4682 (2006).

40. S. Honary and H. Orafai, The effect of different plasticizer molecular weights and concentrations on mechanical and thermomechanical properties of free films. *Drug Dev. Ind. Pharm.* **28,** 711–715 (2002).

41. T.D. Stark, H. Choi and P.W. Diebel, Influence of plasticizer molecular weight on plasticizer retention in PVC geomembranes. *Geosynth. Int.* **12,** 99–110 (2005).

42. A.J. Nijenhuis, E. Colstee, D.W. Grijpma, and A.J. Pennings, High molecular weight poly(L-lactide) and poly(ethylene oxide) blends: Thermal characterization and physical properties. *Polymer* **37,** 5849–5857 (1996).

43. S. Saeidlou, M.A. Huneault, H.B. Li, and C.B. Park, Poly(lactic acid) crystallization. *Prog. Polym. Sci.* **37,** 1657–1677 (2012).